Supporting Information

Synthesis of ^{14}N and ^{15}N-labeled trityl-nitroxide biradicals with strong spin-spin interaction and improved sensitivity to redox status and oxygen

Yangping Liu,[†] Frederick A. Villamena,[†,‡] Yuguang Song,[†] Jian Sun,[†]

Antal Rockenbauer[§] and Jay L. Zweier[†,*]

[†]*Center for Biomedical EPR Spectroscopy and Imaging, The Davis Heart and Lung Research Institute, the Division of Cardiovascular Medicine, Department of Internal Medicine and* [‡]*Department of Pharmacology, College of Medicine, The Ohio State University, Columbus, OH, 43210, USA,* [§]*Chemical Research Center, Institute of Structural Chemistry, P.O. Box 17, H-1525 Budapest, Hungary.*

* Email: Jay.Zweier@osumc.edu

Supplementary Materials Table of Contents

I. The purity analysis of TNN14 and TNN15 with HPLC

Briefly, 20 μl of 200 μM TNN14 and TNN15 were injected separately into the HPLC system (CoulArray System from ESA Analytical, Ltd. Chelmsford, MA) on a Supelcosil LC-18-T column (4.6 x 150 mm, 3 micron, Sigma) with automated gradient controller, refrigerated autosampler, and ESA software for data collection and analysis. The mobile phase consists of the medium A containing 20 mM ammonium acetate (pH 7.0) and medium B containing 20 mM ammonium acetate: methanol : acetonitrile = 40 : 20 : 40 (v : v : v) (pH 7.0) at a flow rate of 1.0 ml/min. Gradient applied was: 0 ~ 3min, 40% B; 3 ~ 18 min, 80% B; 18 ~ 28min, 85% B; 28 ~ 30min, 40% B; followed by 15 min equilibration of 40% B before next injection. The compounds were detected at 469 nm by the UV-Vis detector serially connected to the column. Under experimental conditions, only two isomers of each compound were detected with the intensity ratio of approximately 1:3 for TNN14 and 1:2 for TNN15. The retention time is 22.63 min for Isomer 1 of TNN14, 23.42 min for Isomer 2 of TNN14, 22.52 min for Isomer 1 of TNN15 and 23.34 min for Isomer 2 of TNN15.

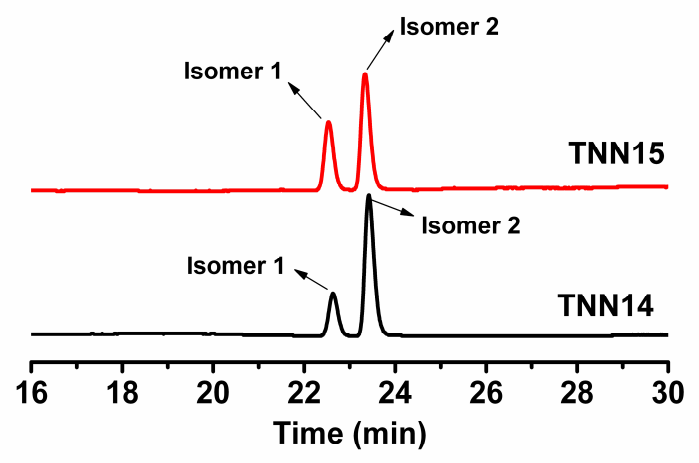

Figure S1. HPLC chromatograms of TNN14 and TNN15.

II. The purity analysis of TNN14 and TNN15 using TEMPOL

The biradical purity was determined using TEMPOL as standard. In a typical experiment, purified trityl-nitroxide biradical as a tricarboxylic acid forms was weighed and dissolved in aqueous solution of NaOH (20 mM). The EPR spectrum was obtained and peak area was determined using double integration. The concentration of the biradical was then determined using a standard curve of known concentration of TEMPOL versus peak area (Figure S2). Each experiment was done in triplicate. The paramagnetic purity for TNN14 and TNN15 was determined to 97 ± 1% and 95 ± 1%, respectively.

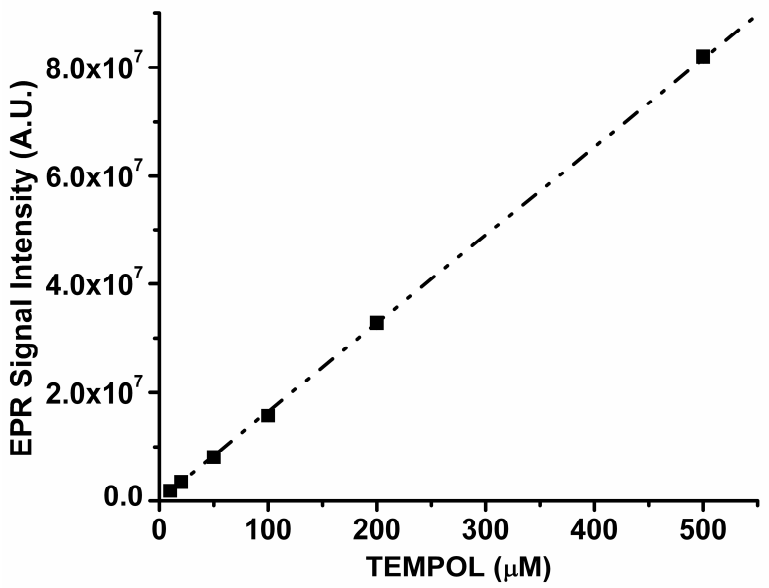

Figure S2. The EPR signal integration of TEMPOL as a function of the concentration in water.

III. EPR simulations

The fitting routine to determine J was previously described with minor revision (Chem. Comm. 2010, 628-630). Briefly, the line broadening caused by the g- and hf anisotropy due to the rotational tumbling is taken into account by the relaxation formula $W(M)=\alpha + \beta*M+\gamma*M*M$. Since the hf lines are broadened by the same extent due to the zero-field interaction, this effect gives contribution only to parameter α. Due to the molecular vibrations and conformational jumps, the J value has a distribution, which is also considered as a broadening factor. The ROKI\EPR program was used to optimize the above relaxation parameters, J and ΔJ values, as well as the g- factors and hf constants. The original program was extended to determine the line positions and transition probabilities by diagonalizing the 2*2 spin Hamiltonian including the Zeeman term, the hf couplings and exchanged coupling. The variation of line position was calculated by the ΔJ distribution of J. The quadratic error between experimental and calculated spectra was minimized, but we could not find further improvement exceeding the noise when J was larger than 400 G.

IV. Concentration effect on the spectra of TNN14

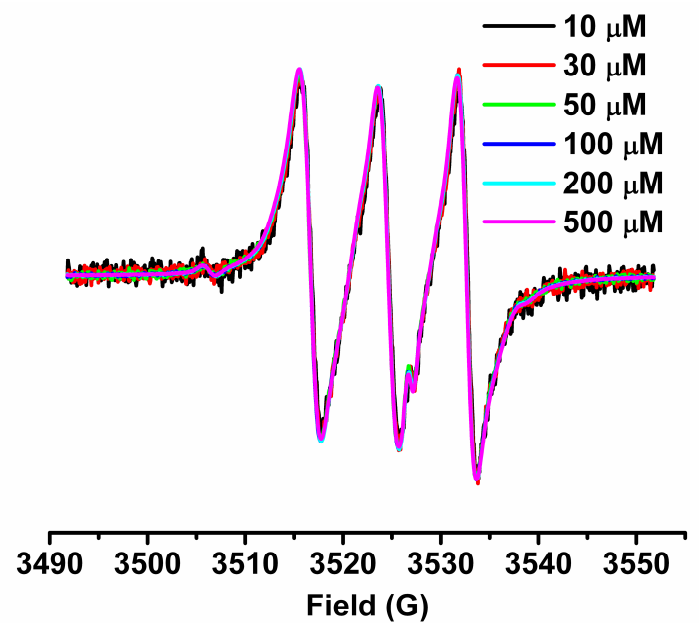

Figure S3. EPR spectra of TNN14 at different concentrations in PBS (pH 7.4, 20 mM) at room temperature. The spectra were scaled to the same maximum lineheight.

V. Reversibility of redox reaction of TNN14

25 μL of the TNN14 solution (100 uM) was mixed with 25 μL of the ascobate solution (2 mM) in PBS (pH 7.4, 50 mM) at room temperature. The solution was divided into two aliquots after 30 min in which 25 μL of water and 25 μL of the $Na_3Fe(CN)_6$ solution (20 mM) were added, respectively, and then EPR spectra were recorded. As a comparison, EPR spectra were recorded on the solution containing only TNN14. The EPR signal of TNN14 was completely restored by $Na_3Fe(CN)_6$ after reaction with ascorbate (Figure S4), implying that the redox reaction of TNN14 is reversible.

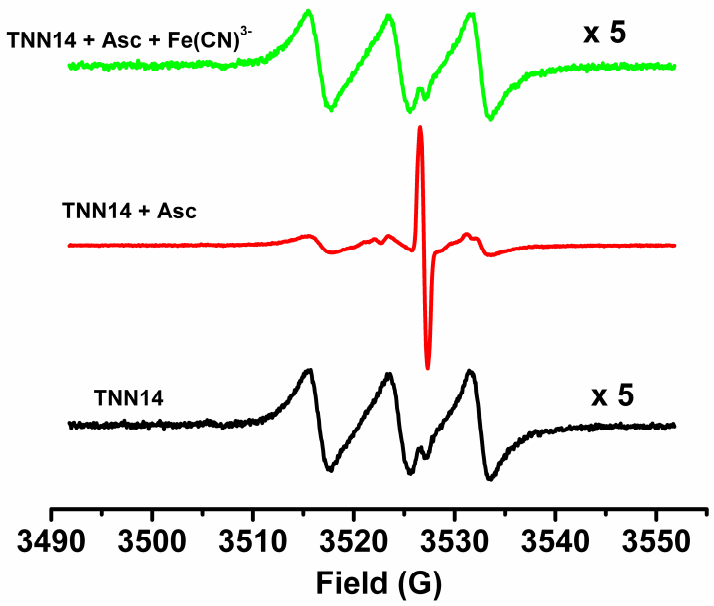

Figure S4. EPR spectra of the TNN14 solution (50 μM) in the presence or absence of ascorbate (1 mM) and $Na_3Fe(CN)_6$ (10 mM).

VI. Reaction of TNN14 with ascorbic acid detected by UV-Vis spectroscopy

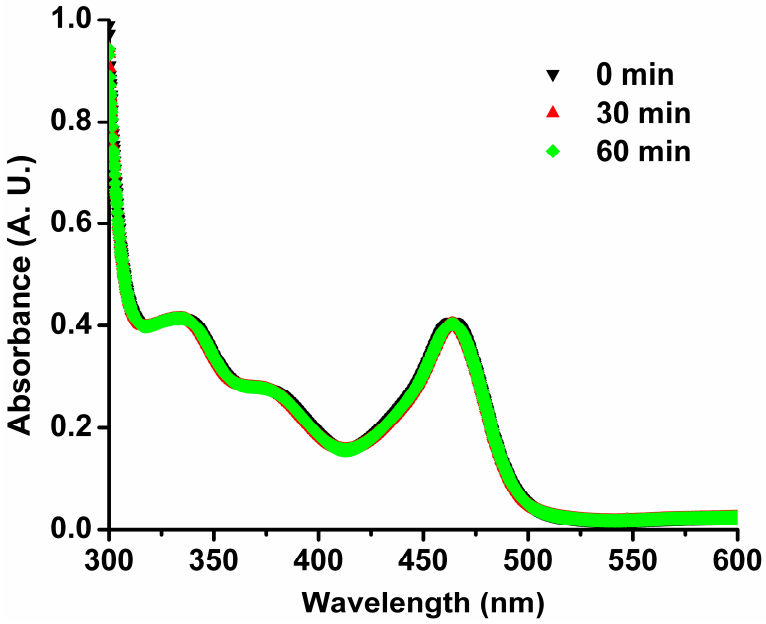

Figure S5. UV-Vis spectra of the reaction solution containing TNN14 (20 μM) and

ascorbate (1 mM). The spectra were recorded at 0, 30 and 60 min after ascorbate was added to the TNN14 solution in PBS (pH 7.4, 20 mM).

VII. Kinetic study of 3-AP with ascorbic acid detected by EPR spectroscopy

Various concentrations of ascorbic acid (1, 2, 4 and 8 mM) were added to the solution of 3-AP (50 μM) in PBS (50 mM, pH 7.4). Incremental EPR spectra were recorded 60 s after mixing and this point was considered to be t = 0 in Figure S1 and S2. Since the ascorbic acid concentration (1, 2, 4 and 8 mM) used was in greater excess than the 3-AP concentration (50 μM), the reaction kinetics of the biradical with ascorbic acid is a pseudo first-order reaction. The rate laws for this reaction are shown below:

$$\mathrm{N} + \mathrm{Asc} \xrightarrow{k_2} \mathrm{NH}$$

$$-\frac{d[N]}{dt} = k_2[Asc][N]$$

$$k_{obs} = k_2[Asc]$$

$$\int \frac{d[N]}{dt} = \int -k_{obs}[N]$$

$$\ln\left(\frac{[N]}{[N]_0}\right) = -k_{obs}t$$

where [N] is the concentration of 3-AP; k_2 is the second-order rate constant; [Asc] is the ascorbic acid concentration used; $[N]_0$ is the initial concentration of 3-AP (e.g., 50 μM). The approximated second-order rate constant k_2 was finally calculated from the slope of the plot of k_{obs} versus [Asc]. The standard deviation for k_2 was obtained from the various points shown in plots S3.

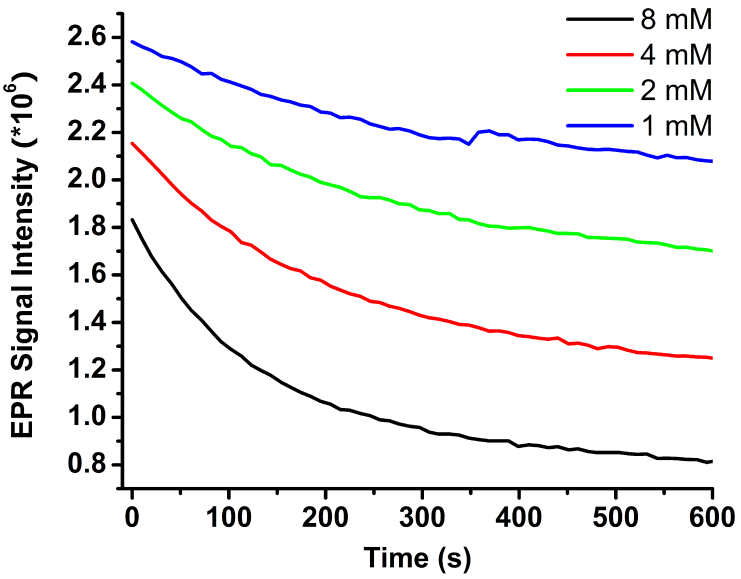

Figure S6. Decay kinetics of 3-AP in the presence of various concentrations of ascorbic acid.

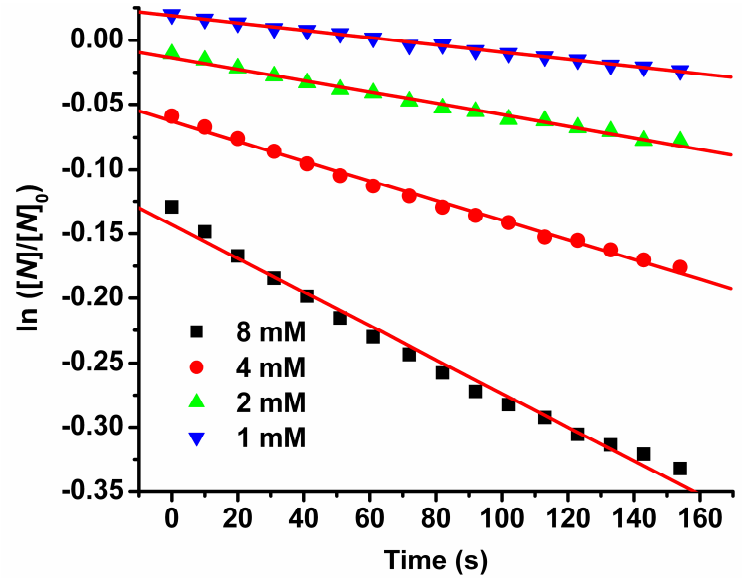

Figure S7. Plot of ln([*N*]/ [*N*]$_0$) as a function of *t* for 3-AP

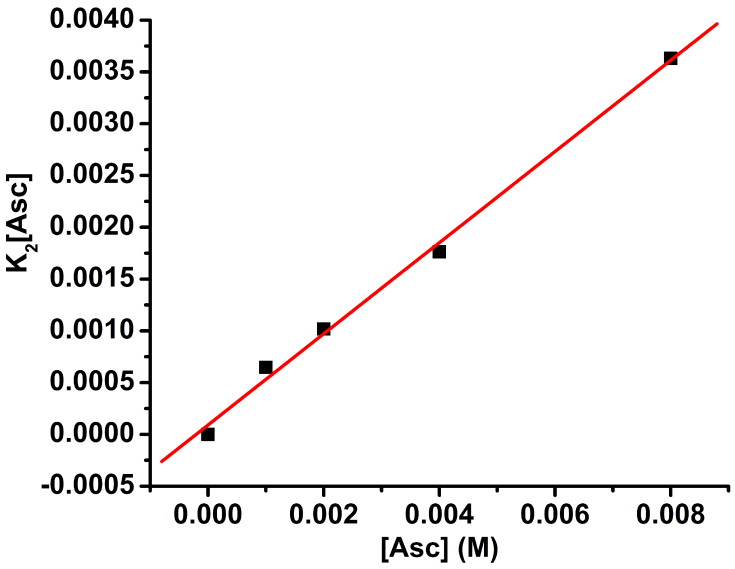

Figure S8. Plot of K_2[Asc] *vs* [Asc] using data shown in Figure S7.

VIII. Spectroscopic characterization

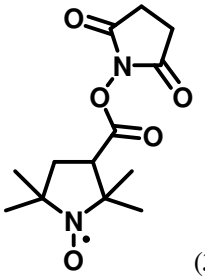

(3-CP-OSu)

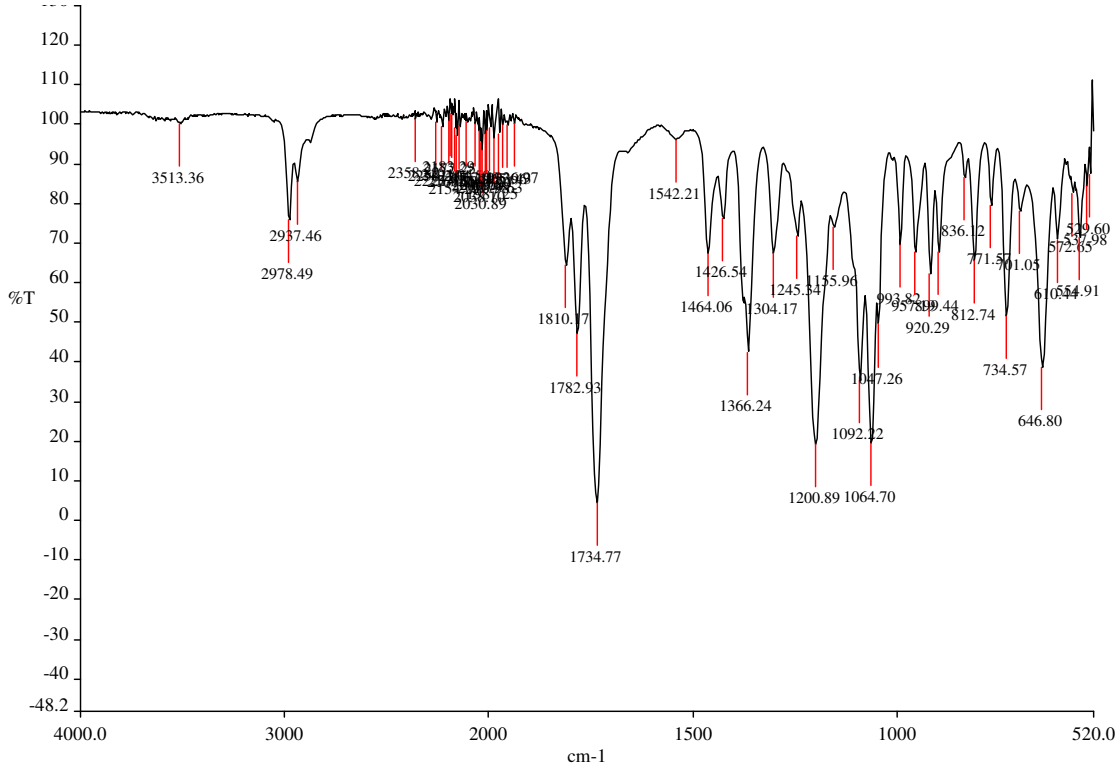

Figure S9. IR spectrum of 3-CP-OSu

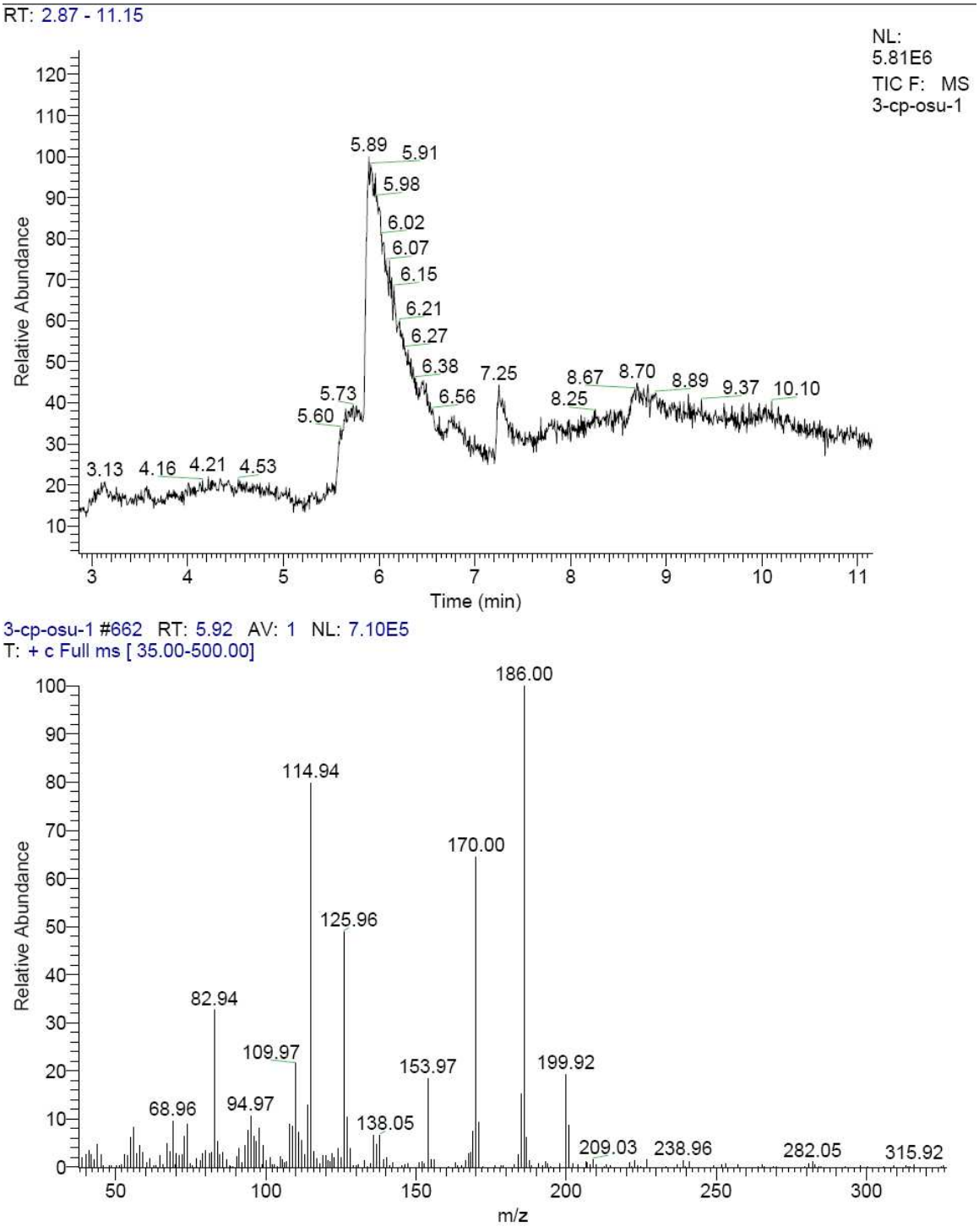

Figure S10. GC-MS spectrum of **3-CP-OSu**

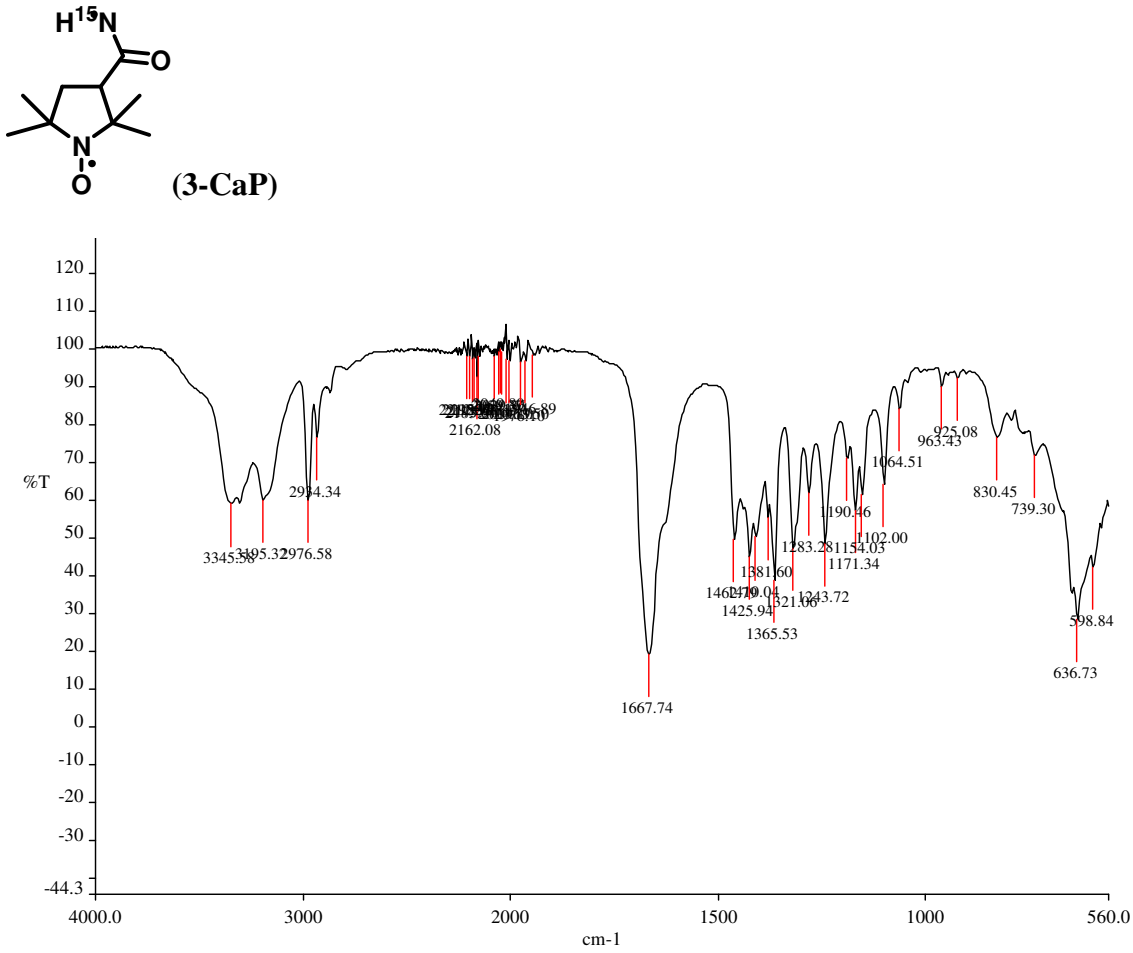

Figure S11. IR spectrum of 3-CaP

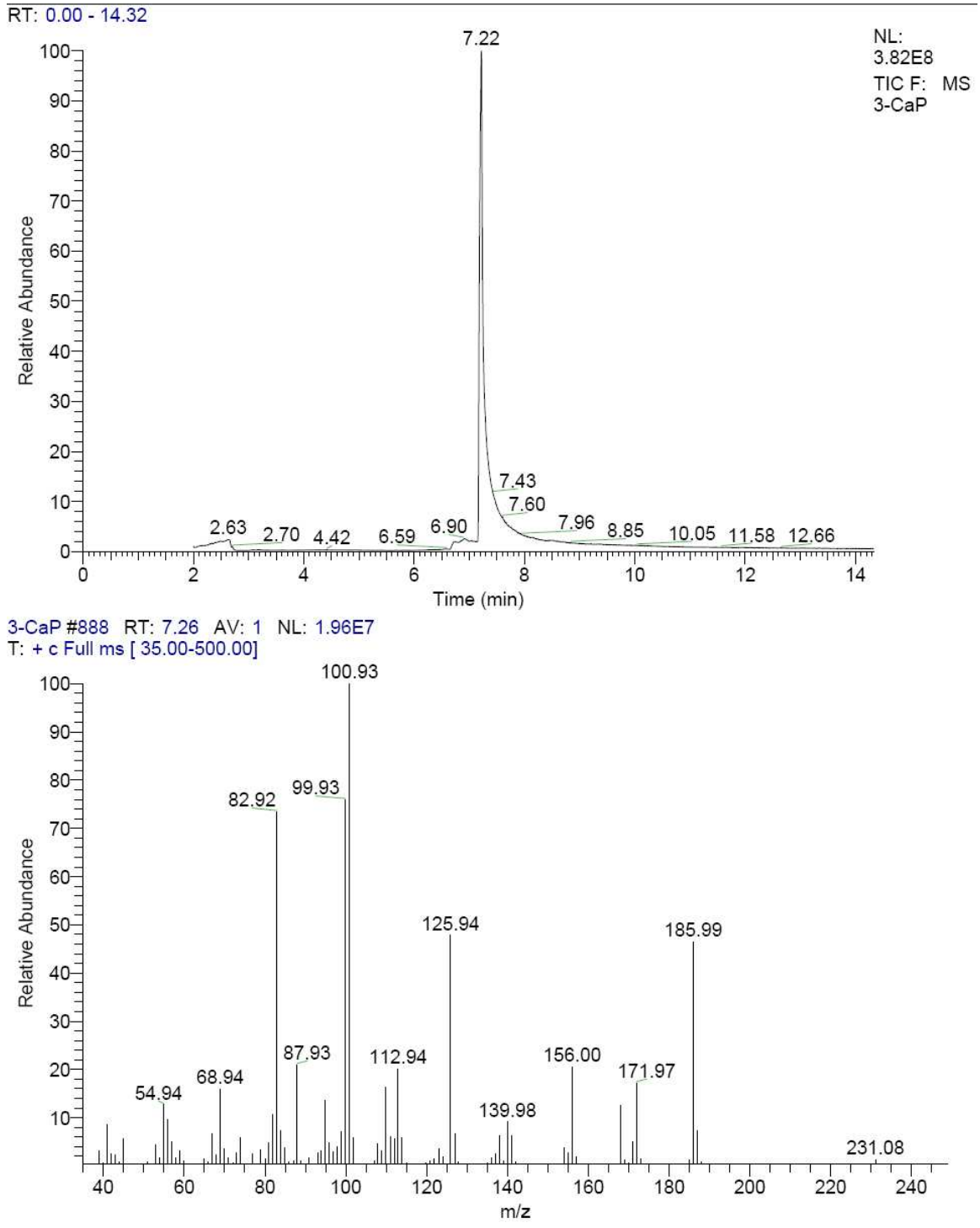

Figure S12. GC-MS spectrum of 3-CaP

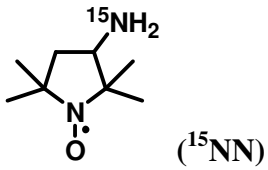

(15NN)

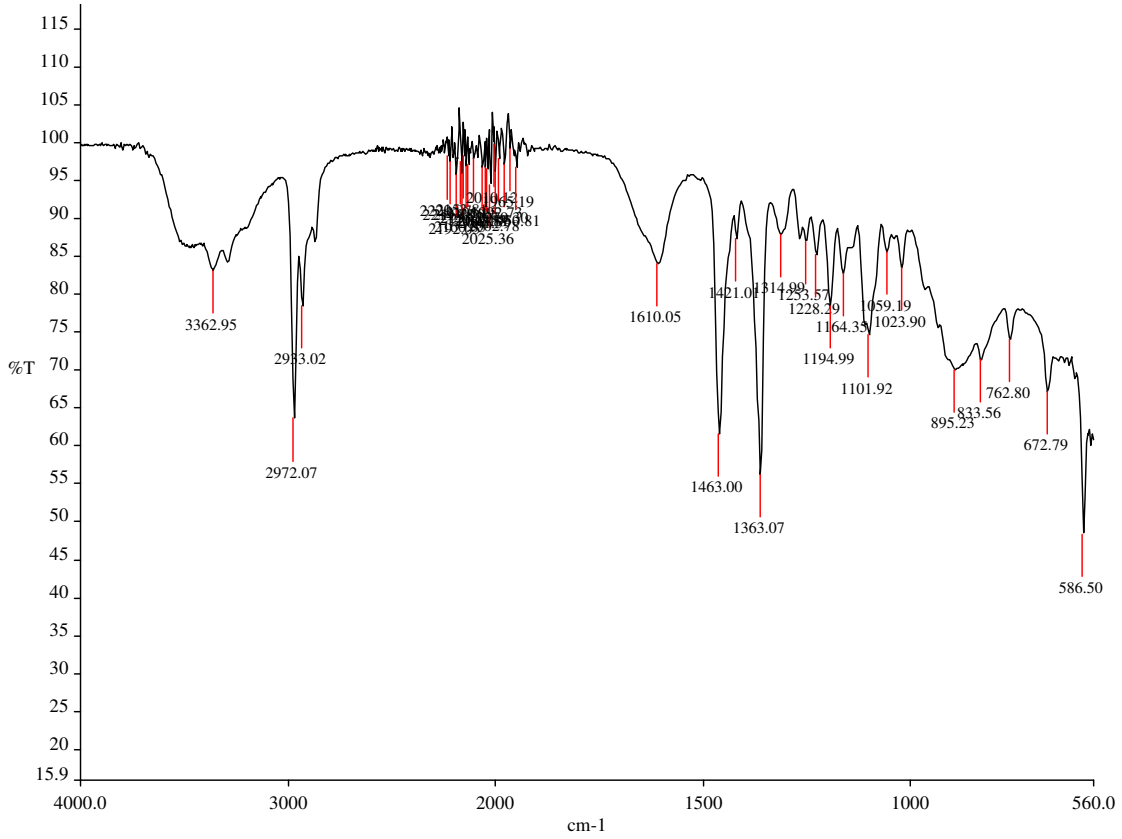

Figure S13. IR spectrum of ^{15}NN

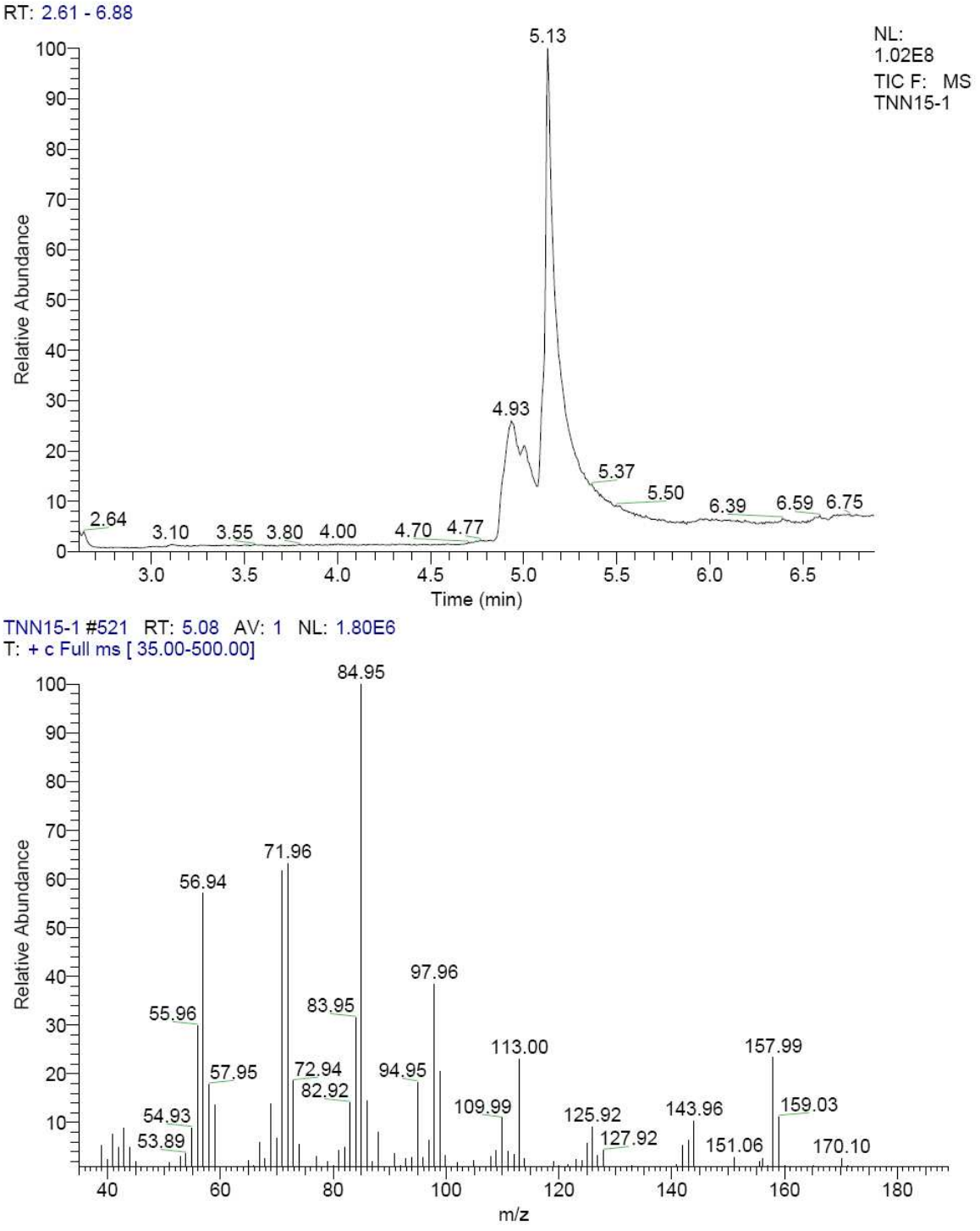

Figure S14. GC-MS spectrum of ^{15}NN

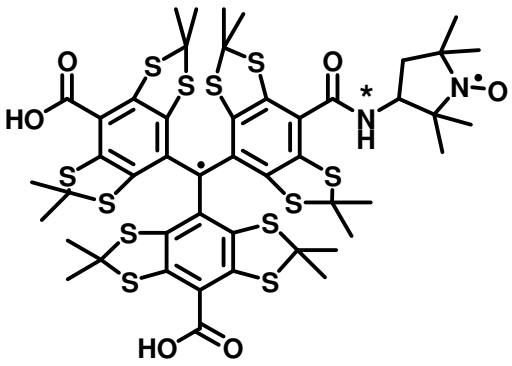

TNN14, *N = ^{14}N

TNN15, *N = ^{15}N

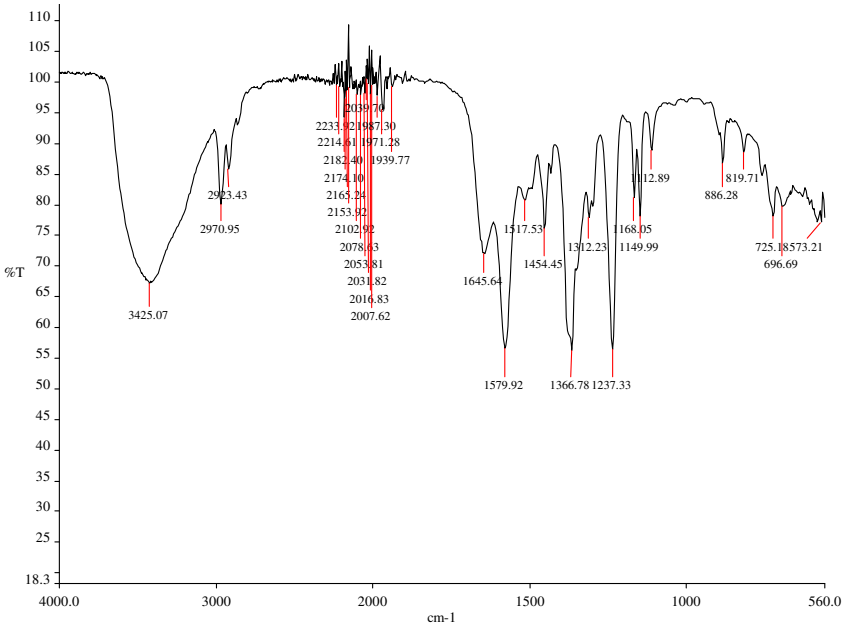

Figure S15. IR spectrum of TNN14

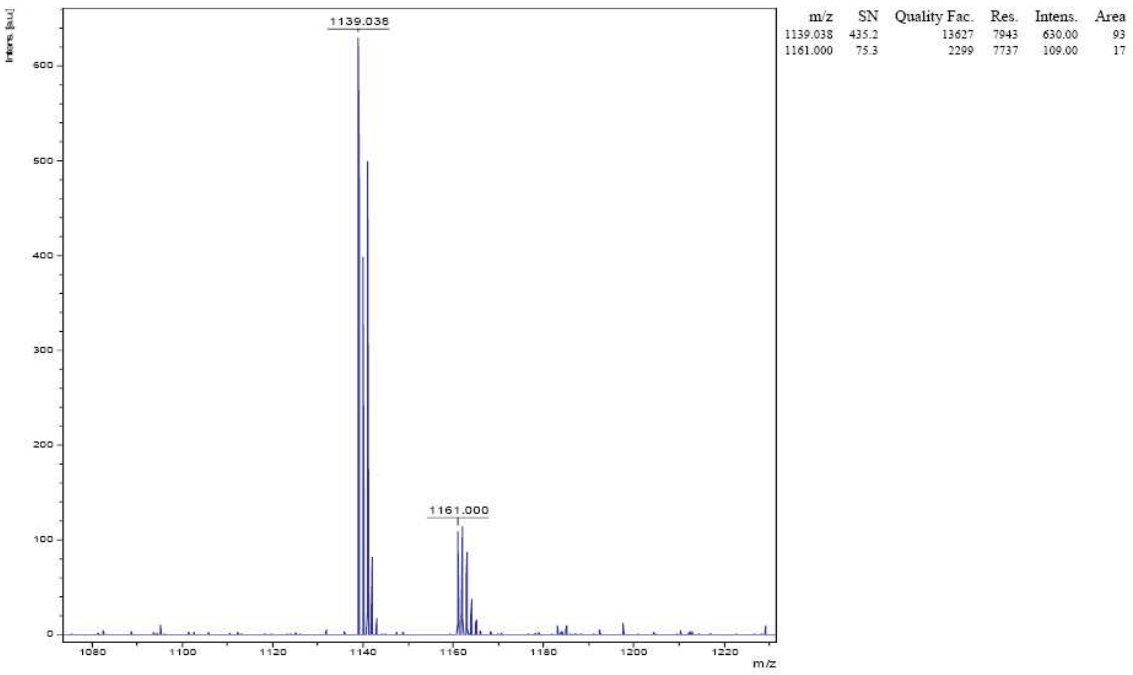

Figure S16. High Resolution Mass Spectrum of TNN14

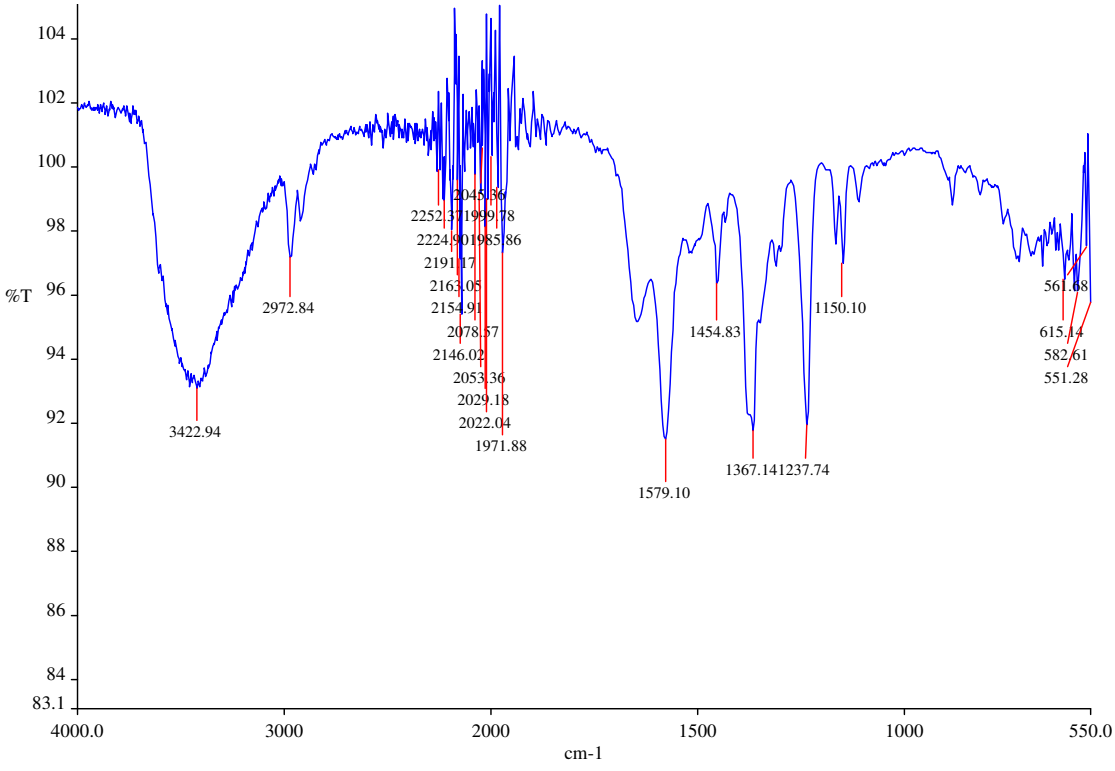

Figure S17. IR spectrum of TNN15

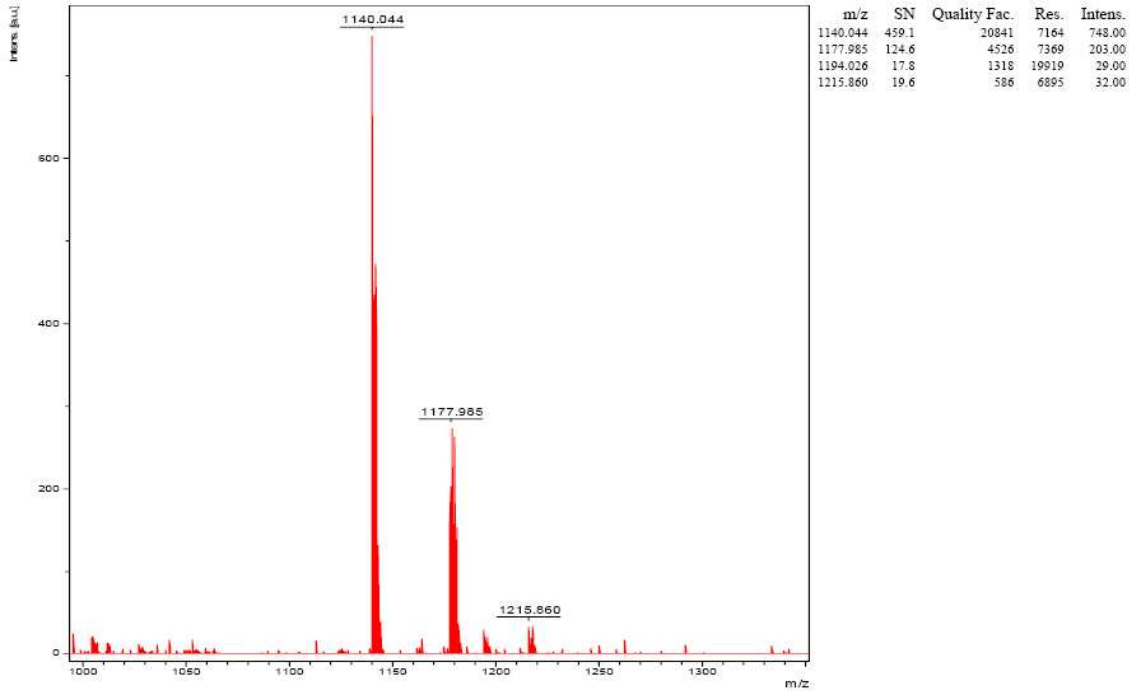

Figure S18. High Resolution Mass Spectrum of TNN15

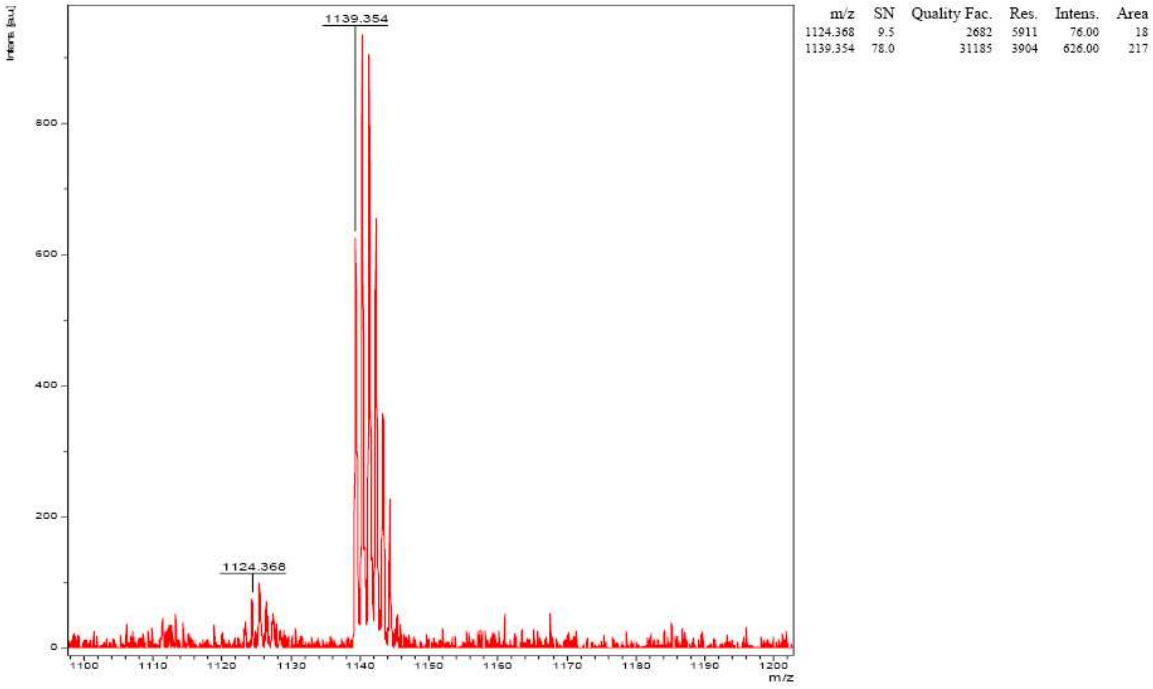

Figure S19. High Resolution Mass Spectrum of TNN14 isomer 1

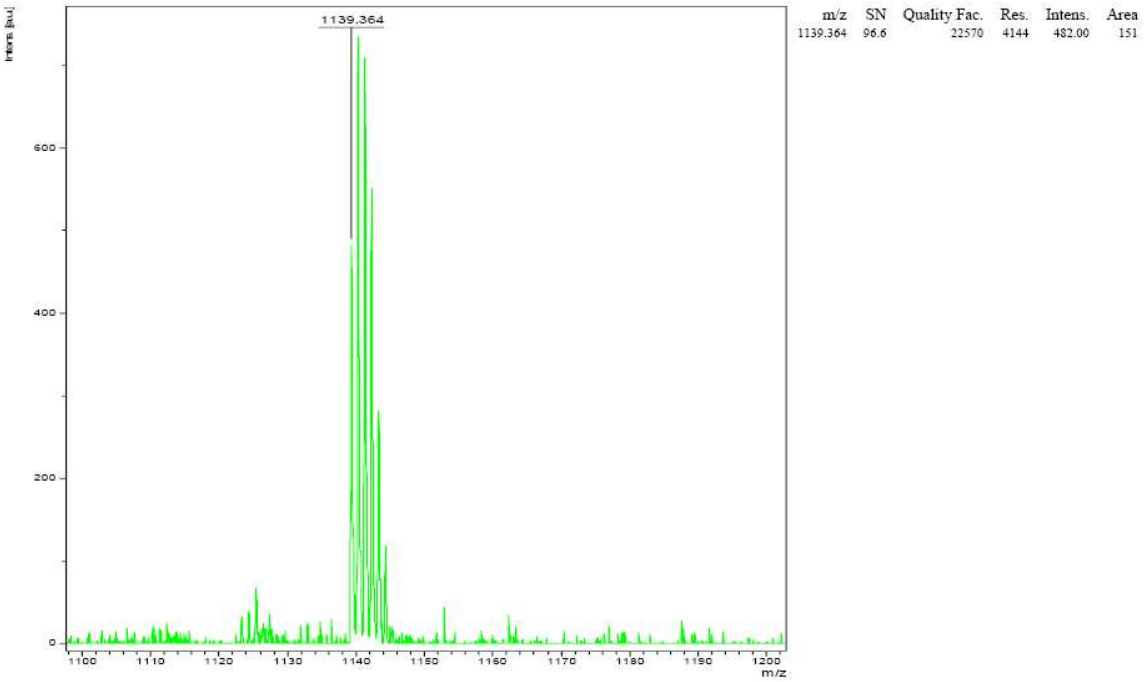

Figure S20. High Resolution Mass Spectrum of TNN14 isomer 2

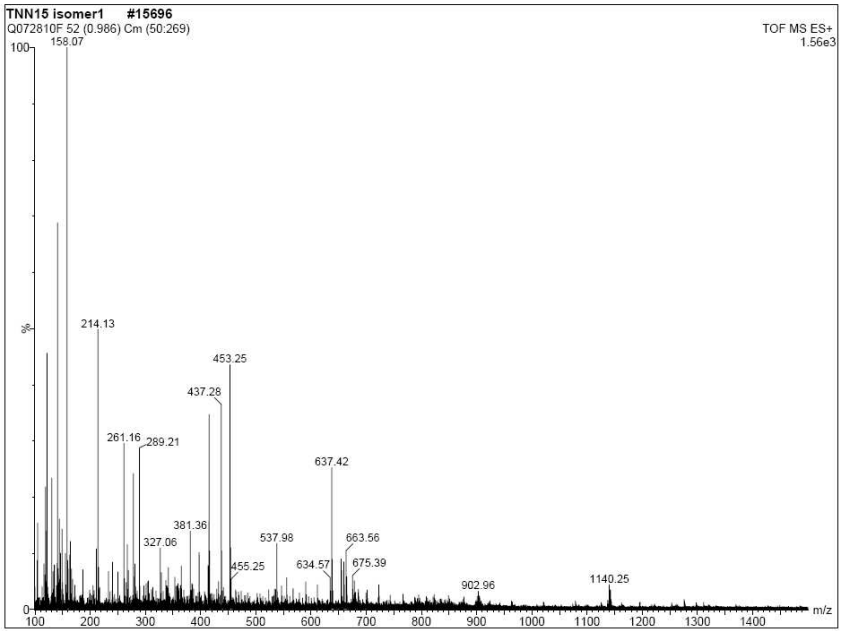

Figure S21. Mass Spectrum of TNN15 isomer 1

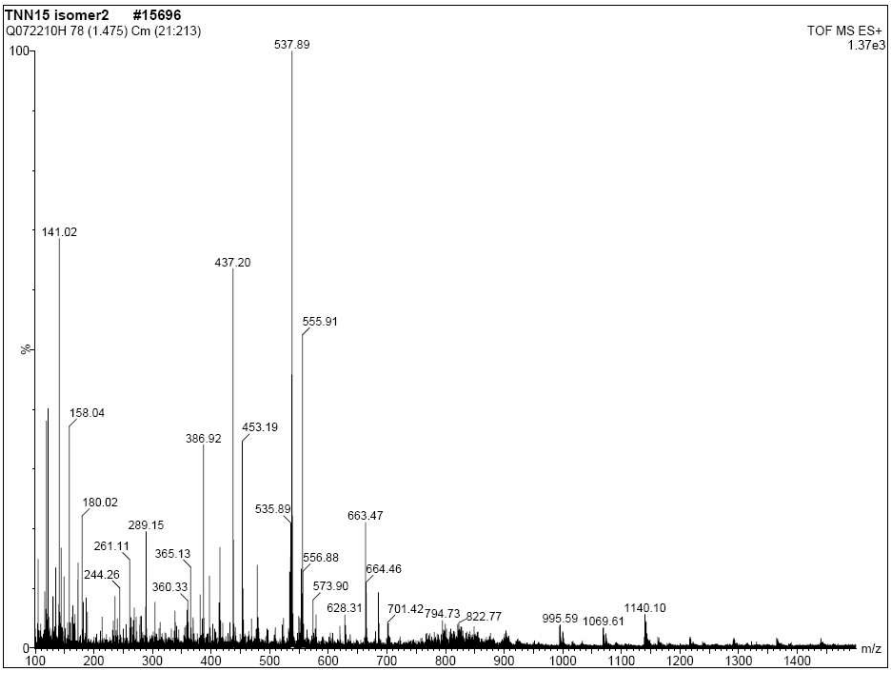

Figure S22. Mass Spectrum of TNN15 isomer 2